Automatic Decomposition of the Clinical Electromyogram

KEVIN C. McGILL, MEMBER, IEEE, KENNETH L. CUMMINS, MEMBER, IEEE, AND LESLIE J. DORFMAN

Abstract—**We describe a new, automatic signal-processing method (ADEMG) for extracting motor-unit action potentials (MUAP's) from the electromyographic interference pattern for clinical diagnostic purposes. The method employs digital filtering to select the spike components of the MUAP's from the background activity, identifies the spikes by template matching, averages the MUAP waveforms from the raw signal using the identified spikes as triggers, and measures their amplitudes, durations, rise rates, numbers of phases, and firing rates. Efficient new algorithms are used to align and compare spikes and to eliminate interference from the MUAP averages. In a typical 10-s signal recorded from the biceps brachii muscle using a needle electrode during a 20 percent-maximal isometric contraction, the method identifies 8–15 simultaneously active MUAP's and detects 30–70 percent of their occurrences. The analysis time is 90 s on a PDP-11/34A.**

I. Introduction

CLINICAL electromyography is a technique for diagnosing neuromuscular disorders by analyzing the electrical signal recorded from a contracting muscle using a needle electrode. The signal, called an electromyogram (EMG), is made of trains of discrete wavelets called motor-unit action potentials (MUAP's) which result from the repetitive discharges of groups of muscle fibers—the term motor unit referring collectively to one motoneuron and the group of muscle fibers it innervates. Distinct MUAP's can be seen only during weak contractions when few motor units are active. During strong contractions, the MUAP's are so numerous that the EMG becomes a noise-like "interference pattern."

Diagnosis is based on the properties (amplitude, durations, and complexity) of the individual MUAP's—small, fragmented MUAP's indicating muscle-fiber loss in myopathies; large, long-duration MUAP's indicating collateral reinnervation accompanying motoneuron dysfunction in neuropathies [1]—and on the intensity and complexity of the interference pattern—which reflect the pattern of motor-unit recruitment. Most electromyographers still assess these properties qualitatively using an oscilloscope and a loudspeaker.

Quantitation is expected to make EMG analysis more objective, reproducible, and diagnostically sensitive [2]–[5]. Several methods have been developed for quantitatively measuring MUAP properties [1], [6]–[12], but they are limited to weak contractions [less than 5 percent maximum voluntary contraction (MVC)] due to their inability to decompose signals containing more than four or five MUAP's. They are, hence, unable to measure high-threshold MUAP's. The method of LeFever and De Luca [13] can analyze EMG's recorded during strong contractions, but it is too time consuming for clinical use. Studer and Gerber *et al.* [14], [15] recently reported a method capable of accurately decomposing signals containing seven MUAP's. Several methods have also been developed for quantitatively characterizing the interference pattern, e.g., in terms of its turn rate or power spectral density [16]–[25], but they have proven to be neither as physiologically well founded nor as diagnostically sensitive as methods that measure MUAP properties.

This paper describes a new computer program (ADEMG, for automatic decomposition electromyography) which can extract as many as 15 simultaneously active MUAP's from EMG's recorded at strengths up to 30 percent MVC. ADEMG is designed to analyze EMG's recorded during 10-s constant isometric contractions using a standard needle electrode and so to be a convenient adjunct to the conventional qualitative EMG examination. The analysis time is 90 s on a PDP-11/34A computer.

The program achieves its high level of performance through four innovative signal-processing techniques: 1) a fast preprocessing filter which suppresses background noise and transforms the MUAP's into sharp, easily identifiable spikes; 2) an efficient new algorithm for aligning and classifying the spikes which achieves high temporal resolution at a low sampling rate; 3) a method for verifying the identified spike trains based on the regularity of their interspike intervals; and 4) a new algorithm for back-averaging the MUAP waveforms from the raw EMG which eliminates interference caused by other MUAP's.

Section II presents an overview of ADEMG. Sections III–VI discuss the four signal-processing steps. Section VII discusses the program's range and limitations.

II. Overview

The EMG signal is recorded using a standard concentric or monopolar needle electrode during a 10-s constant isometric contraction. Constancy ensures steady MUAP firing patterns and minimizes the chance of electrode slippage. The force of contraction should optimally be a certain fixed percentage of the muscle's full strength to ensure reproducibility and conformity with normative data. Clinical methods are described more fully in [26]. The

Manuscript received June 18, 1984; revised February 25, 1985.

K. C. McGill is with the Rehabilitation Research and Development Center, Veterans Administration Medical Center, Palo Alto, CA 94304.

K. L. Cummins is with Nicolet Biomedical Instruments, Madison, WI 53711.

L. J. Dorfman is with the Department of Neurology, Stanford University School of Medicine, Stanford, CA 94305 and the Rehabilitation Research and Development Center, Veteran's Administration Medical Center, Palo Alto, CA 94304.

0018-9294/85/0700-0470$01.00

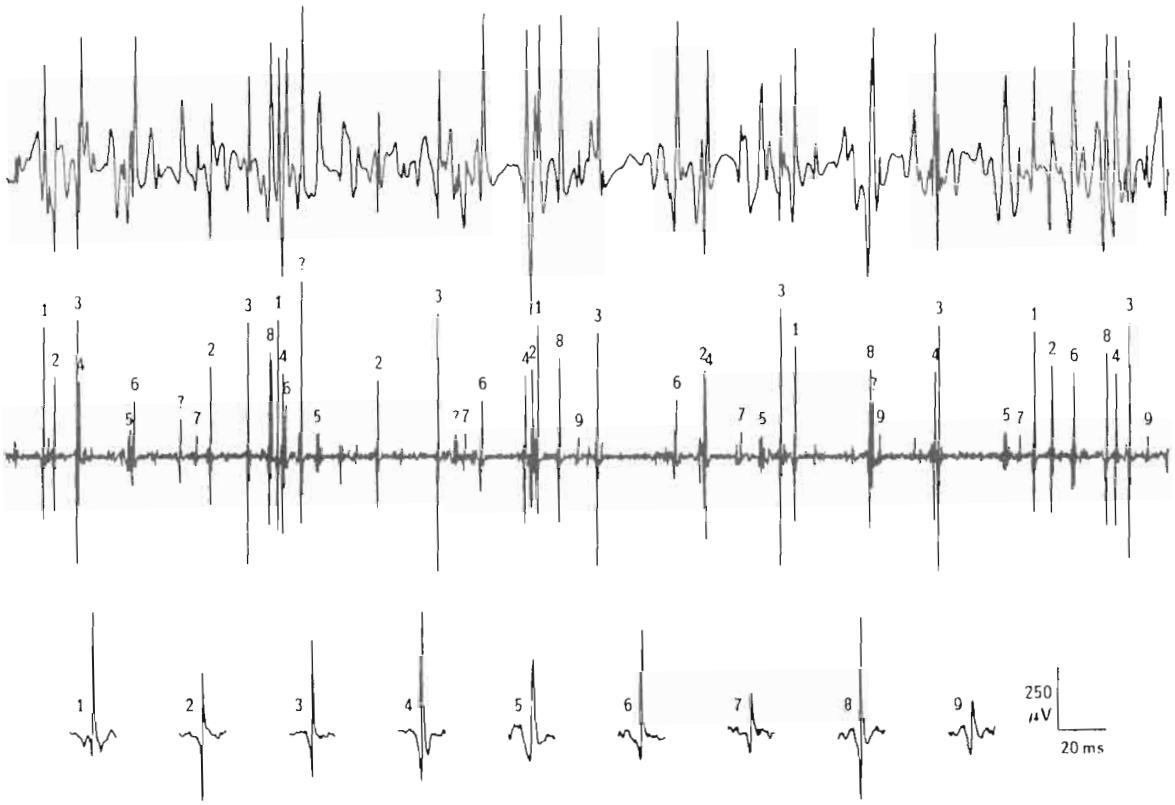

Fig. 1. (Top) Raw EMG segment recorded from biceps brachii using concentric needle electrode—a typical "mixed interference pattern" in which the individual MUAP's are difficult to identify and characterize because of superimpositions. (Middle) Same segment after filtering using the second-order differentiating filter. The identities of the spikes as determined by ADEMG are shown. (Bottom) The MUAP waveforms corresponding to the nine identified spikes.

EMG signal is amplified by a standard electromyograph and band-pass filtered as usual (e.g., 8 Hz–8 kHz). The signal is then antialias filtered at 5 kHz, digitized at 10 kHz, and written to disk for subsequent computer processing.

The signal processing consists of four steps (Figs. 1 and 2): 1) the raw EMG signal is digitally filtered to transform the sharp rising edges of the MUAP's into narrow spikes better suited for detection and classification; 2) the spikes that exceed a certain detection threshold are classified by a one-pass template-matching method which automatically recognizes and forms templates of the recurring spikes; 3) each tentatively identified spike train is verified by examining the regularity of its interspike intervals (ISI's); and 4) the MUAP's corresponding to the verified spike trains are averaged from the raw signal using the identified spikes as triggers.

Finally, the amplitude, duration, number of phases, rise rate, firing rate, and coefficient of ISI variation are estimated for each identified MUAP. Statistics on these variables are accumulated over all recordings from different sites in the same muscle and printed out. Optionally, the MUAP waveforms, ISI histograms, and firing patterns can also be printed out.

III. Prefiltering

MUAP spikes originating from muscle fibers close to the electrode have sharp rising edges while MUAP's originating farther away are broadened due to the low-pass-filtering character of the muscle tissue [27]. As a result, high-pass filtering [13], [28] or differentation [29] is effective in selecting the spikes from the background activity. The effect of such filtering is shown in Fig. 3: the MUAP spikes are accentuated and the background activity is suppressed.

ADEMG uses one of the following two prefilters:

$$x_t = y_{t+1} - y_{t-1} \qquad \text{(first order)} \qquad (1a)$$

$$x_t = y_{t+2} - y_{t+1} - y_t + y_{t-1} \qquad \text{(second order)} \qquad (1b)$$

where y_t is the sampled raw signal and x_t is the sampled filtered signal. These filters belong to a class of so-called "low-pass differentiators" [30] and have the following properties: 1) they are designed for efficient "Nyquist-rate" sampling, 2) they have excellent temporal resolution resulting from their wide bandwidths, and 3) they are very fast, requiring only a few additions and subtractions per sample.

From a time-domain point of view, these filters compute approximations of the first and second derivatives of the input signal and thus accentuate the rapid rising edges of the MUAP's, converting them into narrow monophasic and biphasic spikes, respectively. (Higher order differentiation would produce polyphasic spikes less suitable for detection purposes.) Differentiation is sometimes avoided in signal processing because it unduly accentuates high-

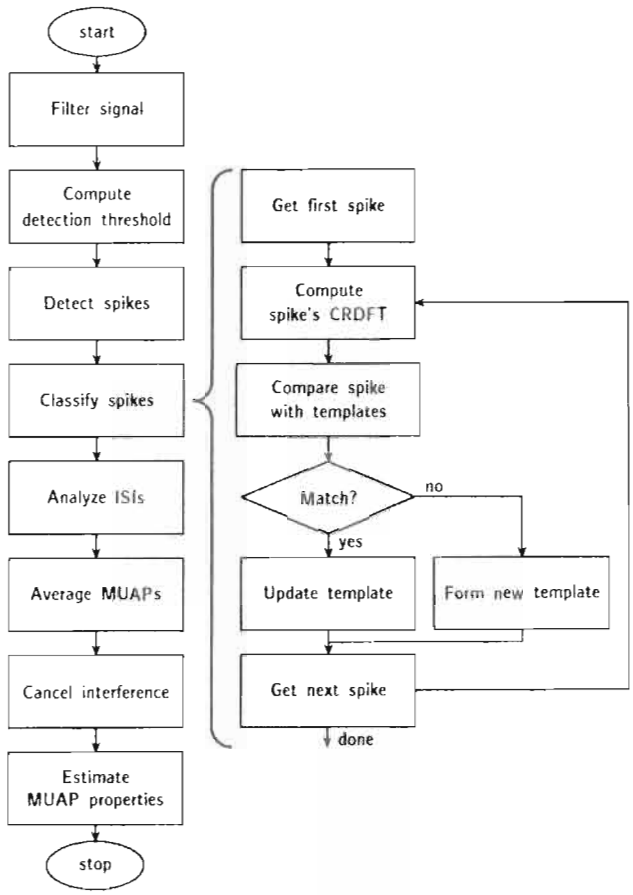

Fig. 2. Flowchart of ADEMG program.

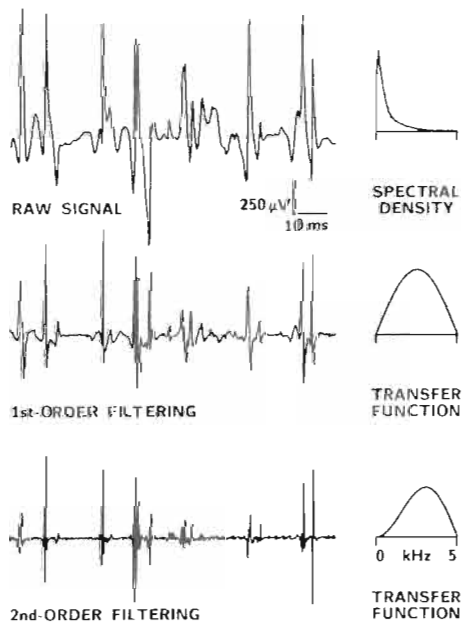

Fig. 3. EMG prefilters. (Top) Raw EMG segment and its power spectral density. (Middle) First-order low-pass differentiator: its effect on the EMG signal and the magnitude of its transfer function. (Bottom) Second-order low-pass differentiator: its effect on the EMG signal and the magnitude of its transfer function.

frequency noise, but it can be performed safely on high-SNR signals with band-limited derivatives by restricting the operation to the frequencies of interest [30]. As Fig. 3 shows, the filters act as differentiators up to only about half the folding frequency and gently cut off above that. Thus, they are tailored for sampling at the Nyquist rate of the MUAP's first or second derivative, respectively.

From a frequency-domain point of view, the filters are band-pass filters which pass the energy from the MUAP's rising edges and suppress the low-frequency background activity and the high-frequency thermal noise.

The spikes in the filtered signal have several advantageous properties that make them easier to work with than the MUAP's in the raw signal. For one thing, they can be reliably detected by a simple threshold-crossing detector. Also, they are quite narrow and can be resolved at close temporal separations. Moreover, they precisely mark the MUAP's times of occurrence and can be used to align the MUAP's for averaging.

Furthermore, despite their narrowness, the spikes are more distinguishable than the MUAP's themselves. This is primarily due to the suppression of low-frequency noise, as can be seen in Fig. 4, which shows ten occurrences of each of three typical MUAP's both before and after filtering. The effect of filtering on distinguishability can be seen quantitatively in the separation matrices [31] of Table I. Each entry shows the separation between a pair of MUAP's as calculated by the formula $E/L^{1/2}\sigma$, where E^2 is the energy of the difference between the waveforms, L is the waveform duration (32 samples), and σ is the rms noise amplitude. A separation of five is necessary for accurate (>95 percent correct) classification [31], [32], and is only achieved after filtering.

IV. Spike Classification

ADEMG identifies the MUAP's in the raw signal by performing template matching on the spikes in the filtered signal.

ADEMG's spike-detection threshold α is set to a coefficient c_1 (typically 3.5) times the standard deviation of the base-line noise. α is computed by solving the following implicit equation which automatically partitions the signal into base-line and nonbase-line components:

$$\alpha = c_1 \left[\sum_{t=1}^{T_1} x_t^2 I(\alpha, t) \Big/ \sum_{t=1}^{T_1} I(\alpha, t) \right]^{1/2} \tag{2a}$$

where x_t is the sampled filtered signal and $I(\alpha, t)$ is the baseline-component indicator function

$$I(\alpha, t) = \begin{cases} 1, & \text{if } |x_t| < \alpha, \\ 0, & \text{otherwise.} \end{cases} \tag{2b}$$

The calculation typically uses only the first 0.2 s of data (i.e., $T_1 = 2000$).

ADEMG detects each spike that exceeds the threshold and, to facilitate spike/template comparisons, computes its canonically registered discrete Fourier transform (CRDFT) [33], [34]. The CRDFT is obtained by first calculating the DFT of the set of samples that make up the spike (32 samples if first-order filtering is used, 16 samples if second order). Then the spike's peak is located with

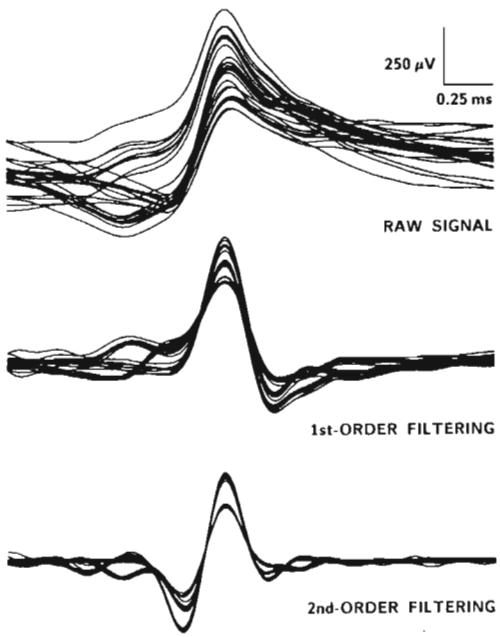

Fig. 4. Ten occurrences each of three MUAP's from the EMG of Fig. 1 after no filtering, first-order filtering, and second-order filtering. The traces are superimposed to show how filtering enhances the distinguishability of the units.

TABLE I
MUAP SEPARATION MATRICES

Unit	2	3	2	3	2	3
1	1.6	2.6	5.2	5.2	10.0	5.5
2		3.9		6.2		7.8
Filter:	none		1st-order		2nd-order	

high temporal resolution by interpolating the trigonometric polynomial specified by the DFT coefficients that approximates the continuous waveform underlying the samples [33]. Finally, the DFT is rotated in a way corresponding to time shifting the peak to the midpoint of the analysis interval. The resulting "canonical" registration is independent of the arbitrary phase of the samples.

The interpolation implicit in the CRDFT representation makes precise spike/template alignment possible when the EMG signal is sampled at its Nyquist rate of 10 kHz. Discrete-time template-matching methods, on the other hand, require oversampling at 5–7 times this rate in order to reduce misalignment errors resulting from time quantization [13], [31]. The slower rate is more efficient since the samples can be written directly to disk without analog-tape buffering and they take up only a fraction of the storage.

Canonical registration implicitly aligns all spikes and templates with one another in a peak-to-peak fashion. This alignment is sufficiently accurate—since the spikes are so narrow—that spikes and templates can be compared directly, without first having to be aligned explicitly as in other template-matching schemes [13], [31]. Table II shows that the peak-to-peak alignment criterion is nearly as accurate as the more commonly used maximum-correlation (least-square error) criterion. The table lists the average increase in template mismatch error for several typical spikes when the peak-to-peak rather than the maximum-correlation criterion is used. Even in the worst case, the increase is only a small fraction of the total error (which is due mostly to background noise).

TABLE II
INCRESE IN MISMATCH ERROR DUE TO PEAK-TO-PEAK ALIGNMENT

Unit	Δe^2
1	1.6 percent
2	1.4
3	4.2
4	7.7
5	1.1
6	4.3
7	2.2
8	5.7
9	2.8

ADEMG performs template matching in the CRDFT domain to avoid the cost of transforming back into the time domain. There are 50 template buffers, each holding one CRDFT. Each new spike is compared to each template using the formula

$$e^2 = \frac{1}{N}|S_0 - X_0|^2 + \frac{2}{N}\sum_{k=1}^{N/2-1}|S_k - X_k|^2 \qquad (3)$$

where X_k, $k = 0, \cdots, N/2 - 1$, is the CRDFT of the spike, S_k is the CRDFT of the template, and N is the spike length (16 or 32 samples). A match occurs if e^2 is less than a certain fraction c_2 (typically 0.1) of the spike's energy. Calculation is streamlined by comparing the sum to the match threshold after each term is added. The energy of the spikes tends to be concentrated in the low-order DFT coefficients; so when the spike and template do not match, the sum usually reaches the threshold after the first few (2–3) terms, and the rest do not have to be computed.

If a match does occur, the template is updated as follows:

$$S_k = (1 - c_3)S_k + c_3X_k, \qquad k = 0,1,\cdots, N/2 - 1 \quad (4)$$

where c_3 is the forgetting factor (typically 0.1) which allows the template to track slow changes in spike shape. If no match occurs, the new spike is stored as a new template, with the least-frequently matched buffers being recycled as needed. Notice that (3) and (4) are essentially identical to their more familiar time-domain counterparts, both in effect and in operation count.

ADEMG does not attempt to resolve superimpositions and so fails to identify every firing of every MUAP. The filtered spikes are usually narrow enough to be identified at separations down to about 1 ms, resulting in identification rates of between 40 and 70 percent.

V. INTERSPIKE INTERVAL ANALYSIS

After the spike trains have been identified, ADEMG examines their firing patterns to verify that they correspond to valid MUAP's.

Motor units fire fairly regularly during constant isometric contractions. Their interspike intervals (ISI's) have an approximately Gaussian distribution whose standard deviation is 10–20 percent of the mean [13], [35]. This regularity can be seen in the ISI histogram of a train identified by ADEMG even when spikes are missing (due to unresolved superimpositions) and erroneous spikes are present (due to misidentifications). A typical ISI histogram is shown in Fig. 5: it has one large mode at the MUAP's true mean ISI, smaller modes at multiples of the true mean ISI due to missing spikes, and two counts at small ISI's due to one erroneous spike. ADEMG uses the ISI histogram to perform the following four steps. (Specific algorithms are presented in [34].)

First, ADEMG identifies and merges together templates that correspond to the same MUAP. The identification is based on similarity of spike shape and regularity of the combined firing pattern of the templates.

Second, ADEMG identifies templates that are time locked to one another. These usually result from complexly shaped MUAP's, including MUAP's with late components, that produce multiple spikes when filtered, each of which is mistakenly identified as a separate unit. From each set of time-locked templates, ADEMG keeps only the one template with the most identified spikes.

Third, ADEMG estimates the following parameters for each train: true mean ISI, coefficient of ISI variation (mean/standard deviation), identification rate (percentage of firings that were identified), and number of erroneous spikes. The train is accepted as valid if there are at least 25 valid spikes, the number of valid spikes exceeds the number of erroneous ones, and the identification rate is greater than 40 percent.

Fourth, ADEMG uses a maximum-*a-posteriori* decision rule to reject the erroneous spikes from the individual valid MUAP trains. This is done in order to improve the accuracy of the waveform averages.

VI. MUAP Averaging

After the MUAP trains have been verified, ADEMG passes back through the raw EMG to average out the MUAP waveforms, using the identified spikes as triggers.

ADEMG first computes the simple MUAP averages as follows:

$$\bar{y}_t^i = \frac{1}{N_i} \sum_{n=1}^{N_i} y_{t_{i,n}+t}, \quad t = -L/2 + 1, \cdots, L/2,$$

$$i = 1, \cdots, M \tag{6}$$

where $\bar{y}^i$ is the simple average of the ith (of M) MUAP, y is the raw signal, $\{t_{i,n}, n = 1, \cdots, N_i\}$ is the list of identified firing times for MUAP i, and L is the averaging length [typically 256 samples (25.6 ms)].

ADEMG then adjusts the simple averages to cancel out the effects of interference from other MUAP's in the following way. A list $\{\tau_{i,j,n}, n = 1, \cdots, N_{i,j}\}$ is compiled for each pair of MUAP's (i,j) containing the offsets between them every time they interfere (i.e., occur within $L/2$ samples of each other). Then the averages are adjusted as follows:

$$\hat{y}_T^i = \bar{y}_t^i - \frac{1}{N_i} \sum_{\substack{j=1 \\ j \neq i}}^{M} \sum_{n=1}^{N_{ij}} \bar{y}_{t-\tau_{i,j,n}}^j$$

$$t = -L/2 + 1, \cdots, L/2, \quad i = 1, \cdots, M \tag{7}$$

where $\hat{y}^i$ is the adjusted average of the ith MUAP. Equation (7) is shown in [34] to be a good approximation to the least-squares averaging algorithm we presented previously in the frequency domain [33]. It has the advantages of being computationally faster and of being free from wrap-around problems.

The effect of interference cancellation is shown in Fig. 6 for three MUAP's from the EMG of Fig. 1. The left-hand traces show the simple averages, and the right-hand traces show the adjusted averages. The bottom two traces illustrate the amount of noise still left after averaging: they show "estimates of flat baseline" obtained by averaging 100 L-point-long segments chosen randomly from the

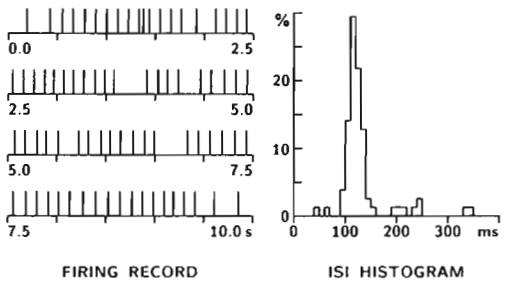

Fig. 5. (Left) MUAP train firing pattern with several missing spikes and one erroneous one. (Right) Histogram of interspike intervals (ISI's).

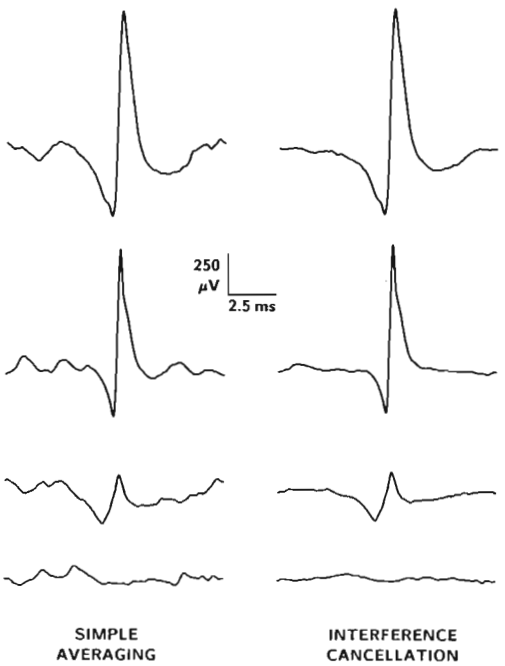

Fig. 6. Average MUAP waveforms for three MUAP's from the EMG of Fig. 1 before and after interference cancellation. The bottom traces are "averages of flat baseline."

EMG signal. The expected value of such an average is zero, and its rms amplitude gives an estimate of the amount of residual noise in the other averages. Interference cancellation typically improves MUAP signal-to-noise ratios by a factor of 2 : 4, and—as seen in Fig. 6—it particularly enhances the low-level beginning and ending portions.

Averaging and interference cancellation are not as severely affected by time quantization as template matching is, and so can be safely performed in discrete time (i.e., sample by sample after alignment to the nearest discrete sampling interval, but without interpolation). The waveforms included in a discrete-time average will be out of phase by amounts randomly distributed in the interval $[-T/2, T/2]$, where T is the sampling interval. The effect is to blur the true average by convolving it with a rectangle function one sampling interval wide or, equivalently, by passing it through a filter whose transfer function is $\sin(\omega T/2)/(\omega T/2)$ [36]. At a sampling rate of 10 kHz, this is a very mild filter whose chief effect is to reduce MUAP amplitudes by a few tenths of a percent. Time quantization of the offsets τ results in incomplete cancellation, but this effect is minimal when N_i is large (>30).

VII. Discussion

ADEMG has been programmed on a PDP-11/34A minicomputer with an FP-11 floating-point processor at the Stanford EMG Laboratory. The program is written in Fortran, with the computation-intensive subroutines coded in assembly language. The program has been optimized for speed and can analyze a 10-s record in 90 s. The program's ability to accurately identify MUAP's, track their firing patterns, and extract their waveforms has been demonstrated by two experiments involving independent checks on MUAP behavior [26], [34]. Its robustness has been demonstrated by its reliability in our preliminary data-gathering studies [26], [37].

Preliminary experience has shown that ADEMG performs very well on signals with sharp MUAP's and low background noise. The signal's acceptability can be judged at recording time by its sharp oscilloscope appearance and its crisp sound, indicating that the electrode's lead-off surface is in direct contact with muscle fibers rather than connective tissue. Some care is needed in selecting a recording site, but not the precise optimization needed in classical MUAP analysis [1]. ADEMG can analyze signals with up to 8–15 simultaneously active MUAP's—corresponding to a force level of 20–40 percent MVC. Above this, the noise and interference are too great and performance deteriorates.

ADEMG's performance is illustrated in Fig. 7, which shows MUAP waveforms obtained from the same site in the biceps brachii muscle at 7, 15, and 30 percent MVC. Seven MUAP's were identified at 7 percent MVC, and all but one were tracked at the higher contractions (MUAP 1 was lost in the noise at 30 percent MVC). Three additional MUAP's were identified at 15 percent MVC, and another three at 30 percent MVC. These later-recruited MUAP's

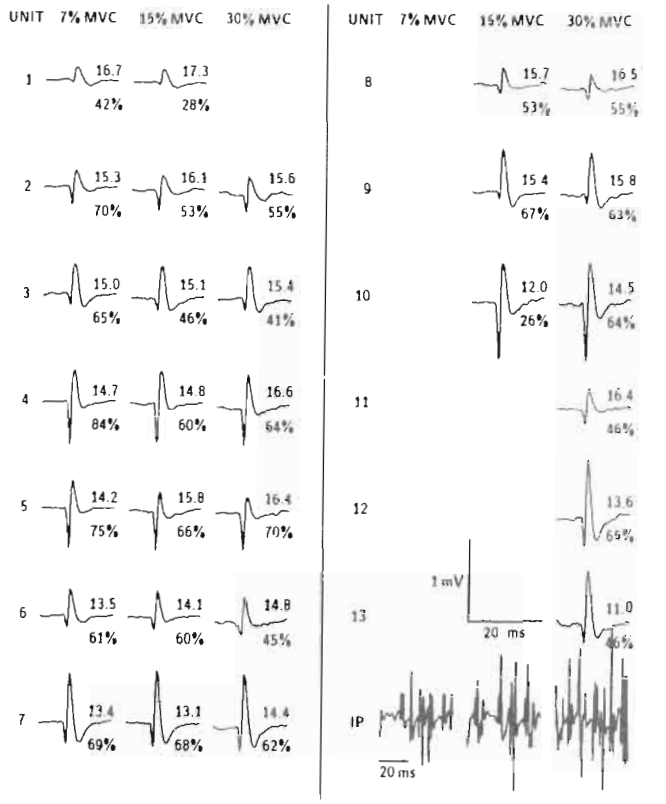

Fig. 7. MUAP's recorded from the same site in the biceps brachii at three different levels of contraction. With each MUAP are shown its firing rate in hertz (above) and its identification rate (below). Segments of raw EMG are also shown for each level of contraction.

are particularly interesting because they could not have been identified by other MUAP analysis methods. The numbers in Fig. 7 indicate each MUAP's firing rate (above) and identification rate (below). The identification rates depend on spike size and noise level but are typically between 40 and 70 percent, even during heavy interference. These rates are sufficient for accurate estimation of the MUAP waveforms, as shown by the consistency of the estimates obtained at the different force levels. Standard errors are typically <5 percent for amplitude, rise rate, and firing rate estimates, and <20 percent for duration.

One important reason for ADEMG's performance is the use of the filtered spikes for classification rather than the MUAP's themselves. The spikes exhibit less interference—they can be distinguished at separations down to 1 ms, an interval at which the MUAP's are superimposed. They also have higher signal-to-noise ratios, particularly during moderately strong contractions with considerable low-frequency background noise. These factors make it possible to decompose signals containing as many as 15 MUAP's. They also make it possible to achieve reliable spike classification using a fast, automatic one-pass template-matching technique (cf. the interactive clustering technique in [15]). Moreover, they ensure adequate identification rates without the need to resolve superimpositions. (Methods for resolving superimpositions are discussed in [34], but they increase computation time unacceptably.)

Another important reason for high performance is the use of constant isometric contractions. This ensures steady firing rates so that firing parameters can be estimated from imperfectly identified MUAP trains. It also lessens the likelihood of electrode slippage and hence of changes in spike shape. ADEMG uses a simple "forgetting average" (4) to track gradual changes (cf. the optimal method in [14]), but we find that when the electrode is held carefully spike shapes usually change very little throughout an entire recording, and sometimes, as in Fig. 7, from one recording to another. When substantial slippage does occur, it can usually be detected at recording time by a change in the signal's sound.

Comparison of results obtained using ADEMG to those obtained using other analysis methods must take into account the fact that ADEMG is biased toward MUAP's with rapid rising or falling edges (< 1.6 ms rise times) and may fail to detect MUAP's of considerable amplitude if they have slower rise times.

In conclusion, ADEMG promises to be a powerful addition to the electromyographer's armamentarium. ADEMG decomposes conventionally recorded EMG signals into their fundamental physiological components: the MUAP's and their firing patterns. It can handle signals from contractions up to 30 percent maximal force (15 simultaneously active MUAP's), making it possible to collect a large number of MUAP's quite quickly and, for the first time, to base clinical diagnosis on the properties of later-recruited MUAP's.

References

[1] F. Buchthal, *An Introduction to Electromyography*. Copenhagen, Denmark: Gyldendal, 1969.

[2] D. C. Boyd, P. J. A. Bratty, and P. D. Lawrence, "A review of the methods of automatic analysis in clinical electromyography," *Comput. Biol. Med.*, vol. 6, pp. 179–190, 1976.

[3] A. Eberstein and J.Goodgold, "Computer analysis in clinical electromyography," *Amer. J. Phys. Med.*, vol. 57, pp. 77–83, 1978.

[4] E. K. Richfield, B. A. Cohen, and J. W. Albers, "Review of quantitative and automated needle electromyographic analyses," *IEEE Trans. Biomed. Eng.*, vol. BME-28, pp. 506–514, 1981.

[5] *Computer-Aided Electromyography*, J. E. Desmedt, Ed. Basel, Switzerland: Karger, 1983.

[6] J. Bergmans, "Computer-assisted measurement of the parameters of single motor unit potentials in human electromyography," in *New Developments in Electromyography and Clinical Neurophysiology*, vol. 2, J. E. Desmedt, Ed. Basel, Switzerland: Karger, 1973, pp. 482–488.

[7] R. G. Lee and D. G. White, "Computer analysis of motor unit action potentials in routine clinical electromyography," in *New Developments in Electromyography and Clinical Neurophysiology*, vol. 2, J. E. Desmedt, Ed. Basel, Switzerland: Karger, 1973, pp. 454–461.

[8] V. J. Prochazka and H. H. Kornhuber, "On-line multi-unit sorting with resolution of superposition potentials," *Electroencephalogr. Clin. Neurophysiol.*, vol. 34, pp. 91–93, 1973.

[9] L. J. Leifer and P. Pinelli, "Analysis of motor units by computer aided electromyography," in *Proc. 3rd Int. Congr. Electrophysiol. Kinesiol.*, Pavia, Italy, 1976, pp. 1–14.

[10] P. Guiheneuc, J. Calamel, C. Doncarli, D. Gitton, and C. Michel, "Automatic detection and pattern recognition of single motor unit potentials in needle EMG," in *Computer-Aided Electromyography*, J. E. Desmedt, Ed. Basel, Switzerland: Karger, 1983, pp. 73–127.

[11] I. Hausmanowa-Petrusewicz and J.Kopec, "Quantitative EMG and its automation," in *Computer-Aided Electromyography*, J. E. Desmedt, Ed. Basel, Switzerland: Karger, 1983, pp. 164–185.

[12] J.-L. Coatrieux, "On-line electromyographic signal processing system," *IEEE Trans. Biomed. Eng.*, vol. BME-31, pp. 199–207, Feb. 1984.

[13] R. S. LeFever and C. J. De Luca, "A procedure for decomposing the myoelectric signal into its constituent action potentials," *IEEE Trans. Biomed. Eng.*, vol. BME-29, pp. 149–157, 1982.

[14] R. M. Studer, R. J. P. de Figueiredo, and G. S. Moschytz, "An algorithm for sequential signal estimation and system identification for EMG signals," *IEEE Trans. Biomed. Eng.*, vol. BME-31, pp. 285–295, Mar. 1984.

[15] A. Gerber, R. M. Studer, R. J. P. de Figueiredo, and G. S. Moschytz, "A new framework and computer program for quantitative EMG signal analysis," *IEEE Trans. Biomed. Eng.*, vol. BME-31, pp. 857–863, Dec. 1984.

[16] A. Moosa, B. H. Brown, and V. Dubowitz, "Quantitative electromyography: Carrier detection in Duchenne type muscular dystrophy using a new automatic technique," *J. Neurol. Neurosurg. Psychiat.*, vol. 35, pp. 841–844, 1972.

[17] A. Magora and B. Gonen, "Computer analysis of the relation between duration and degree of superposition of electromyographic spikes," *Electromyography*, vol. 17, pp. 83–98, 1977.

[18] A. Touraine, S. Bajada, and D. Dollfus-Samson, "Analyse automatique de l'electromyogramme: Technique et resultats chez des sujets sain et des malades," *Electroencephalogr. Clin. Neurophysiol.*, vol. 49, pp. 646–651, 1980.

[19] R. G. Willison, "Analysis of electrical activity in healthy and dystrophic muscle in man," *J. Neurol. Neurosurg. Psychiat.*, vol. 27, pp. 386–394, 1964.

[20] A. Fuglsang-Frederiksen and A. Mansson, "Analysis of electrical activity of normal muscle in man at different degrees of voluntary effort," *J. Neurol. Neurosurg. Psychiat.*, vol. 38, pp. 683–694, 1975.

[21] A. Blinowska, J. Verroust, and G. Cannet, "The determination of motor unit characteristics from the low frequency electromyographic power spectra," *Electromyogr. Clin. Neurophysiol.*, vol. 19, pp. 281–290, 1979.

[22] J.-L. Coatrieux, "Interference electromyogram processing," *Electromyogr. Clin. Neurophysiol.*, vol. 23, pp. 229–242, 1983.

[23] J. N. Walton, "The electromyogram in myopathy: Analysis with the audio-frequency spectrometer," *J. Neurol. Neurosurg. Psychiat.*, vol. 15, pp. 219–226, 1952.

[24] J. W. Gersten, F. S. Cenkovich, and G. D. Jones, "Harmonic analysis of normal and abnormal electromyograms," *Amer. J. Phys. Med.*, vol. 4, pp. 235–240, 1965.

[25] L.-E. Larsson, "On the relation between the EMG frequency spectrum and the duration of symptoms in lesions of the peripheral motor neuron," *Electroencephalogr. Clin. Neurophysiol.*, vol. 38, pp. 69–78, 1975.

[26] K. C. McGill and L. J. Dorfman, "Automatic decomposition electromyography (ADEMG): Validation and normative data in biceps brachii," *Electroencephalogr. Clin. Neurophysiol.*, in press.

[27] P. Rosenfalck, "Intra- and extracellular potential fields of active nerve and muscle fibers," *Acta Physiol. Scand.*, vol. 61, suppl. 226, pp. 1–96, 1964.

[28] I. Gath and E. Stålberg, "Techniques for improving the selectivity of electromyographic recordings," *IEEE Trans. Biomed. Eng.*, vol. BME-26, pp. 467–472, 1979.

[29] S. Andreassen and A. Rosenfalck, "Recording from a single motor unit during strong effort," *IEEE Trans. Biomed. Eng.*, vol. BME-25, pp. 501–508, 1978.

[30] S. Usui and I. Amidror, "Digital low-pass differentiation for biological signal processing," *IEEE Trans. Biomed. Eng.*, vol. BME-29, pp. 686–693, 1982.

[31] B. C. Wheeler and W. J. Heetderks, "A comparison of techniques for classification of multiple neural signals," *IEEE Trans. Biomed. Eng.*, vol. BME-29, pp. 752–759, 1982.

[32] W. J. Heetderks, "Criteria for evaluating multiunit spike separation techniques," *Biol. Cyber.*, vol. 29, pp. 215–220, 1979.

[33] K. C. McGill and L. J. Dorfman, "High-resolution alignment of sampled waveforms," *IEEE Trans. Biomed. Eng.*, vol. BME-31, pp. 462–468, June 1984.

[34] K. C. McGill, "A method for quantitating the clinical electromyogram," Ph.D. dissertation, Stanford Univ., Stanford, CA, 1984.

[35] C. J. De Luca, "Physiology and mathematics of myoelectric signals," *IEEE Trans. Biomed. Eng.*, vol. BME-26, pp. 313–325, 1979.

[36] W. M. Roberts and D. K. Hartline, "Multi-channel nerve impulse

separation techniques," in *Computer Technology in Neuroscience*, P. B. Brown, Ed. New York: Wiley, 1976.
[37] L. J. Dorfman and K. C. McGill, "Automatic analysis of motor unit action potential properties during strong muscular contractions using ADEMG," in *Proc. 31st Annu. Meet. Amer. Assoc. Electromyogr. Electrodiagnosis*, 1984.

Kevin C. McGill (M'84) received the A.B., B.S.E.E., and M.S.E.E. degrees from the University of Notre Dame, Notre Dame, IN, in 1974, 1975, and 1979, respectively, and the Ph.D. degree in electrical engineering from Stanford University, Stanford, CA, in 1984.

Since 1983 he has been working as a Biomedical Engineer at the Rehabilitation Research and Development Center, Palo Alto VA Medical Center, Palo Alto, CA. His research interests include biomedical signal processing and the quantitative analysis of electromyograms.

Kenneth L. Cummins (S'73–M'78), for a photograph and biography, see p. 438 of the June 1985 issue of this TRANSACTIONS.

Leslie J. Dorfman is an Associate Professor of Neurology and (by courtesy) of Mechanical Engineering at Stanford University, Stanford, CA. He directs the Laboratories of Electromyography and Sensory Evoked Potentials at Stanford University Medical Center, where he also supervises the Adult Neuromuscular Diseases Service. He also serves as Program Medical Director of the Neural and Muscular Systems Group at the Rehabilitation Research and Development Center, Palo Alto VA Medical Center, Palo Alto, CA. His main research interest is the application of signal processing techniques in clinical neurophysiology for diagnosis of neurological disorders and for neurological rehabilitation.